

Comparison of the Legacy and Gold SnIa Dataset Constraints on Dark Energy Models

S. Nesseris^a and L. Perivolaropoulos^b

Department of Physics, University of Ioannina, Greece

^a e-mail: me01629@cc.uoi.gr, ^b e-mail: leandros@cc.uoi.gr

(Dated: February 3, 2008)

We have performed a comparative analysis of three recent and reliable SnIa datasets available in the literature: the Full Gold (FG) dataset (157 data points $0 < z < 1.75$), a Truncated Gold (TG) dataset (140 data points $0 < z < 1$) and the most recent Supernova Legacy Survey (SNLS) dataset (115 data points $0 < z < 1$). We have analyzed and compared the likelihood of cosmological constant and dynamical dark energy parametrizations allowing for crossing of the phantom divide line (PDL). We find that even though the constraints obtained using the three datasets are consistent with each other at the 95% confidence level, the latest (SNLS) dataset shows distinct trends which are not shared by the Gold datasets. We find that the best fit dynamical $w(z)$ obtained from the SNLS dataset does not cross the PDL $w = -1$ and remains above and close to the $w = -1$ line for the whole redshift range $0 < z < 1$ showing no evidence for phantom behavior. The LCDM parameter values ($w_0 = -1$, $w_1 = 0$) almost coincide with the best fit parameters of the dynamical $w(z)$ parametrizations. In contrast, the best fit dynamical $w(z)$ obtained from the Gold datasets (FG and TG) clearly crosses the PDL and departs significantly from the PDL $w = -1$ line while the LCDM parameter values are about 2σ away from the best fit $w(z)$. In addition, the $(\Omega_{0m}, \Omega_\Lambda)$ parameters in a LCDM parametrization without a flat prior, fit by the SNLS dataset, favor the minimal flat LCDM concordance model. The corresponding fit with the Gold datasets mildly favors a closed universe and the flat LCDM parameter values are $1\sigma - 2\sigma$ away from the best fit $(\Omega_{0m}, \Omega_\Lambda)$.

PACS numbers: 98.80.Es, 98.65.Dx, 98.62.Sb

I. INTRODUCTION

Current cosmological observations show strong evidence that we live in a spatially flat universe [1] with low matter density [2] that is currently undergoing accelerated cosmic expansion [3, 4, 5]. The most direct indication for the current accelerating expansion comes from the accumulating type Ia supernovae (SnIa) data [4, 5] which provide a detailed form of the recent expansion history of the universe.

This accelerating expansion has been attributed to a dark energy [6] component with negative pressure which can induce repulsive gravity and thus cause accelerated expansion.

The simplest and most obvious candidate for this dark energy is the cosmological constant Λ [7] with equation of state $w = p/\rho = -1$. This model however raises theoretical problems related to the fine tuned value required for the cosmological constant [7]. These difficulties have lead to a large variety of proposed models where the dark energy component evolves with time [8] usually due to an evolving scalar field (quintessence) which may be minimally [8] or non-minimally [9] coupled to gravity. The main prediction of the dynamical models is the evolution of the dark energy density parameter $\Omega_X(z)$. Combining this prediction with the prior assumption for the matter density parameter Ω_{0m} , the predicted expansion history $H(z)$ is obtained as

$$H(z)^2 = H_0^2[\Omega_{0m}(1+z)^3 + \Omega_X(z)] \quad (1.1)$$

The dark energy density parameter is usually expressed

as

$$\Omega_X(z) = \Omega_{0X}(1+z)^{3(1+w(z))} \quad (1.2)$$

where $w(z)$ is related to $H(z)$ by [10, 11]

$$w(z) = \frac{\frac{2}{3}(1+z)\frac{d\ln H}{dz} - 1}{1 - (\frac{H_0}{H})^2\Omega_{0m}(1+z)^3} \quad (1.3)$$

If the dark energy can be described as an ideal fluid with conserved energy momentum tensor $T^{\mu\nu} = \text{diag}(\rho, p, p, p)$ then the above parameter $w(z)$ is identical with the equation of state parameter of dark energy

$$w(z) = \frac{p(z)}{\rho(z)} \quad (1.4)$$

Independently of its physical origin, the parameter $w(z)$ is an observable derived from $H(z)$ (with prior knowledge of Ω_{0m}) and is usually used to compare theoretical model predictions with observations.

Most evolution behaviors of $w(z)$ can be reproduced by assuming appropriate scalar field quintessence potentials. If however $w(z)$ were observationally found to cross the phantom divide line (PDL) $w = -1$ then all minimally coupled single scalar field models would be ruled out as dark energy candidates [12, 13] (this includes phantom [14] and k -essence models [15]). This would leave only models based on extended gravity theories [16, 17] and combinations of multiple fields [18, 19] (quintessence + phantom) as dark energy candidates. It is therefore important to utilize the available SnIa datasets to place constraints on $w(z)$ and determine the likelihood of having a $w(z)$

that crosses the PDL, as done in Ref.[20] using the Gold dataset following a robust procedure. This paper confirms the evidence for crossing the PDL with $w < -1$ at present and also shows some hint for oscillating $w(z)$ at best fit in agreement with Ref.[11], which were the first to point this trend.

The two most reliable and robust SNIa datasets existing at present are the Gold dataset [4] and the Supernova Legacy Survey (SNLS) [5] dataset. The Gold dataset compiled by Riess et. al. is a set of supernova data from various sources analyzed in a consistent and robust manner with reduced calibration errors arising from systematics. It contains 143 points from previously published data plus 14 points with $z > 1$ discovered recently with the HST. The SNLS is a 5-year survey of SNIa with $z < 1$. It has recently [5] released the first year dataset. The SNLS has adopted a more efficient SNIa search strategy involving a ‘rolling search’ mode where a given field is observed every third or fourth night using a single imaging instrument thus reducing photometric systematic uncertainties. The published first year SNLS dataset consists of 44 previously published nearby SNIa with $0.015 < z < 0.125$ plus 73 distant SNIa ($0.15 < z < 1$) discovered by SNLS two of which are outliers and are not used in the analysis. The fact that in the two datasets a set of low- z SNIa is common to both samples could only lead to minor common systematics due to low redshift.

The above observations provide the apparent magnitude $m(z)$ of the supernovae at peak brightness after implementing correction for galactic extinction, K-correction and light curve width-luminosity correction. The resulting apparent magnitude $m(z)$ is related to the luminosity distance $d_L(z)$ through

$$m_{th}(z) = \bar{M}(M, H_0) + 5\log_{10}(D_L(z)) \quad (1.5)$$

where in a flat cosmological model

$$D_L(z) = (1+z) \int_0^z dz' \frac{H_0}{H(z'; a_1, \dots, a_n)} \quad (1.6)$$

is the Hubble free luminosity distance ($H_0 d_L/c$), a_1, \dots, a_n are theoretical model parameters and \bar{M} is the magnitude zero point offset and depends on the absolute magnitude M and on the present Hubble parameter H_0 as

$$\begin{aligned} \bar{M} &= M + 5\log_{10}\left(\frac{c H_0^{-1}}{Mpc}\right) + 25 = \\ &= M - 5\log_{10}h + 42.38 \end{aligned} \quad (1.7)$$

The parameter M is the absolute magnitude which is assumed to be constant after the above mentioned corrections have been implemented in $m(z)$.

The data points of the Gold dataset are given after the corrections have been implemented, in terms of the distance modulus

$$\mu_{obs}^G(z_i) \equiv m_{obs}^G(z_i) - M \quad (1.8)$$

The SNLS dataset however also presents for each point, the stretch factor s used to calibrate the absolute magnitude and the rest frame color parameter c which mainly

measures host galaxy extinction by dust. Thus, the distance modulus in this case depends apart from the absolute magnitude M , on two additional parameters α and β defined from

$$\mu_{obs}^{SNLS} = m_{obs}^{SNLS}(z_i) - M + \alpha(s_i - 1) - \beta c_i \quad (1.9)$$

which are fit along with the theoretical parameters using a recursive procedure discussed below.

The theoretical model parameters are determined by minimizing the quantity

$$\chi^2(a_1, \dots, a_n) = \sum_{i=1}^N \frac{(\mu_{obs}(z_i) - \mu_{th}(z_i))^2}{\sigma_{\mu i}^2 + \sigma_{int}^2 + \sigma_{v i}^2} \quad (1.10)$$

where $\sigma_{\mu i}^2$, σ_{int}^2 and $\sigma_{v i}^2$ are the errors due to flux uncertainties, intrinsic dispersion of SNIa absolute magnitude and peculiar velocity dispersion respectively. These errors are assumed to be gaussian and uncorrelated. The theoretical distance modulus is defined as

$$\mu_{th}(z_i) \equiv m_{th}(z_i) - M = 5\log_{10}(D_L(z)) + \mu_0 \quad (1.11)$$

where

$$\mu_0 = 42.38 - 5\log_{10}h \quad (1.12)$$

and μ_{obs} is given by (1.8) and (1.9) for the Gold and SNLS datasets respectively.

The steps we followed for the minimization of (1.10) for the Gold and SNLS datasets are described in detail in the Appendix. The validity of our analysis has been verified by comparing the part of our results that overlaps with the results of the original Refs [4, 5] of the Legacy and Gold datasets.

II. COMPARATIVE ANALYSIS

We will consider four representative $H(z)$ parametrizations and minimize the χ^2 of eq. (1.10) with respect to model parameters. We compare the best fit parametrizations obtained with three datasets

- The full SNLS dataset with 115 datapoints (excluding two outliers) and $z < 1$.
- The Full Gold dataset (FG) with 157 datapoints and $0 < z < 1.7$.
- A Truncated version of the Gold dataset (TG) with 140 datapoints and $z < 1$ which can be compared in a more direct way with SNLS.

The four fitted parametrizations include the general LCDM without a flat prior:

$$H(z)^2 = H_0^2[\Omega_{0m}(1+z)^3 + \Omega_\Lambda + (1 - \Omega_{0m} - \Omega_\Lambda)(1+z)^2] \quad (2.1)$$

$$w(z) = -1 \quad (2.2)$$

and three dynamical dark energy parametrizations with two free parameters which allow for crossing of the PDL:

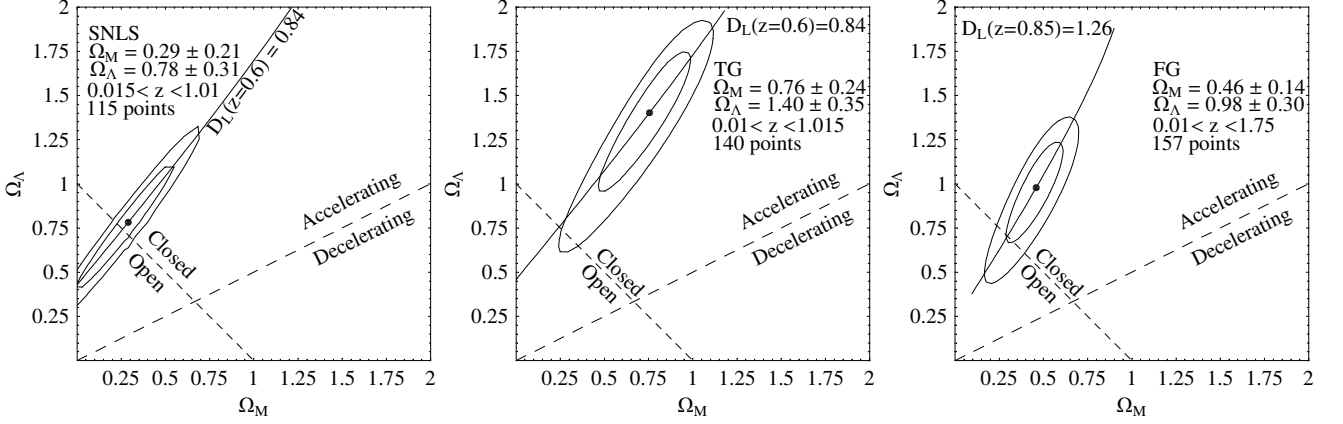


FIG. 1: The 68% and 95% confidence region ellipses in the $\Omega_{0m} - \Omega_\Lambda$ plane based on parametrization (2.1). The three plots correspond to the three datasets discussed in the text (SNLS, TG and FG). Notice that flat LCDM is more favored by the SNLS dataset than by the Gold datasets.

- Parametrization A:

$$w(z) = w_0 + w_1 z \quad (2.3)$$

$$H^2(z) = H_0^2[\Omega_{0m}(1+z)^3 + (1 - \Omega_{0m})(1+z)^{3(1+w_0-w_1)}e^{3w_1z}] \quad (2.4)$$

- Parametrization B:

$$w(z) = w_0 + w_1 \frac{z}{1+z} \quad (2.5)$$

$$H^2(z) = H_0^2[\Omega_{0m}(1+z)^3 + (1 - \Omega_{0m})(1+z)^{3(1+w_0+w_1)}e^{3w_1[1/(1+z)-1]}] \quad (2.6)$$

- Parametrization C:

$$w(z) = \frac{a_1 + 3(\Omega_{0m} - 1) - 2a_1z - a_2(-2 + 2z + z^2)}{3(1 - \Omega_{0m} + a_1z + 2a_2z + a_2z^2)} \quad (2.7)$$

$$H^2(z) = H_0^2[\Omega_{0m}(1+z)^3 + a_1(1+z) + a_2(1+z)^2 + (1 - \Omega_{0m} - a_1 - a_2)] \quad (2.8)$$

The motivation behind parametrization C is to mimic a two-component DE model. Alternatively, it could be viewed as a power law expansion in the scale factor dependence of the DE energy density. In analyzing the general LCDM of eq.(2.1) we used

$$D_L(z) = \frac{(1+z)}{\sqrt{\Omega_{0m} + \Omega_{0X} - 1}} \text{Sin}[\sqrt{\Omega_{0m} + \Omega_{0X} - 1} \int_0^z dz \frac{H_0}{H(z)}] \quad (2.9)$$

instead of eq.(1.6) which is only suitable for flat models.

In Fig. 1 we show the confidence region ellipses in the $\Omega_{0m} - \Omega_\Lambda$ plane based on parametrization (2.1). The three plots correspond to the three datasets discussed above (SNLS, TG and FG). The following comments can be made on these plots:

- The major axes of the elliptic contours are approximately parallel in the three plots. This effect[21] is due to the degeneracy of the fitted $D_L(z; \Omega_{0m}, \Omega_\Lambda)$ with respect to certain linear combinations of the parameters $\Omega_{0m} - \Omega_\Lambda$ in the redshift range of interest. For example, choosing a representative redshift $z = 0.6$ it is easy to show that the value $D_L(z = 0.6) = 0.84$ is obtained by all combinations of $\Omega_{0m} - \Omega_\Lambda$ that satisfy $\Omega_{0m} - 0.80\Omega_\Lambda = -0.38$. The direction of this (approximate) degeneracy line is determined by the $H(z)$ parametrization and the redshift range considered but the actual location of the line is determined by the data.
- The two versions of the Gold dataset favor a closed universe instead of a flat universe ($\Omega_{tot}^{TG} = 2.16 \pm 0.59$, $\Omega_{tot}^{FG} = 1.44 \pm 0.44$). This trend is not realized by the SNLS dataset which gives $\Omega_{tot}^{SNLS} = 1.07 \pm 0.52$.
- The point corresponding to SCDM ($\Omega_{0m}, \Omega_\Lambda$) = (1,0) is ruled out by all datasets at a confidence level more than 10σ .
- The values of μ_0^{min} that minimize the $\chi^2(\Omega_{0m}, \Omega_\Lambda)$ of eq. (1.10) (with $H(z)$ given by (2.1)) obtained by all three datasets are consistent with each other. We find $\mu_0^{SNLS} = 43.15 \pm 0.05$, $\mu_0^{TG} = 43.30 \pm 0.05$ and $\mu_0^{FG} = 43.32 \pm 0.05$. This alleviates the possible discrepancy between high and low redshift data discussed recently in Ref. [21].
- If we use a prior constraint of flatness $\Omega_{0m} + \Omega_\Lambda = 1$ thus restricting on the corresponding dotted line of Fig. 1 and using the parametrization

$$H(z)^2 = H_0^2[\Omega_{0m}(1+z)^2 + (1 - \Omega_{0m})] \quad (2.10)$$

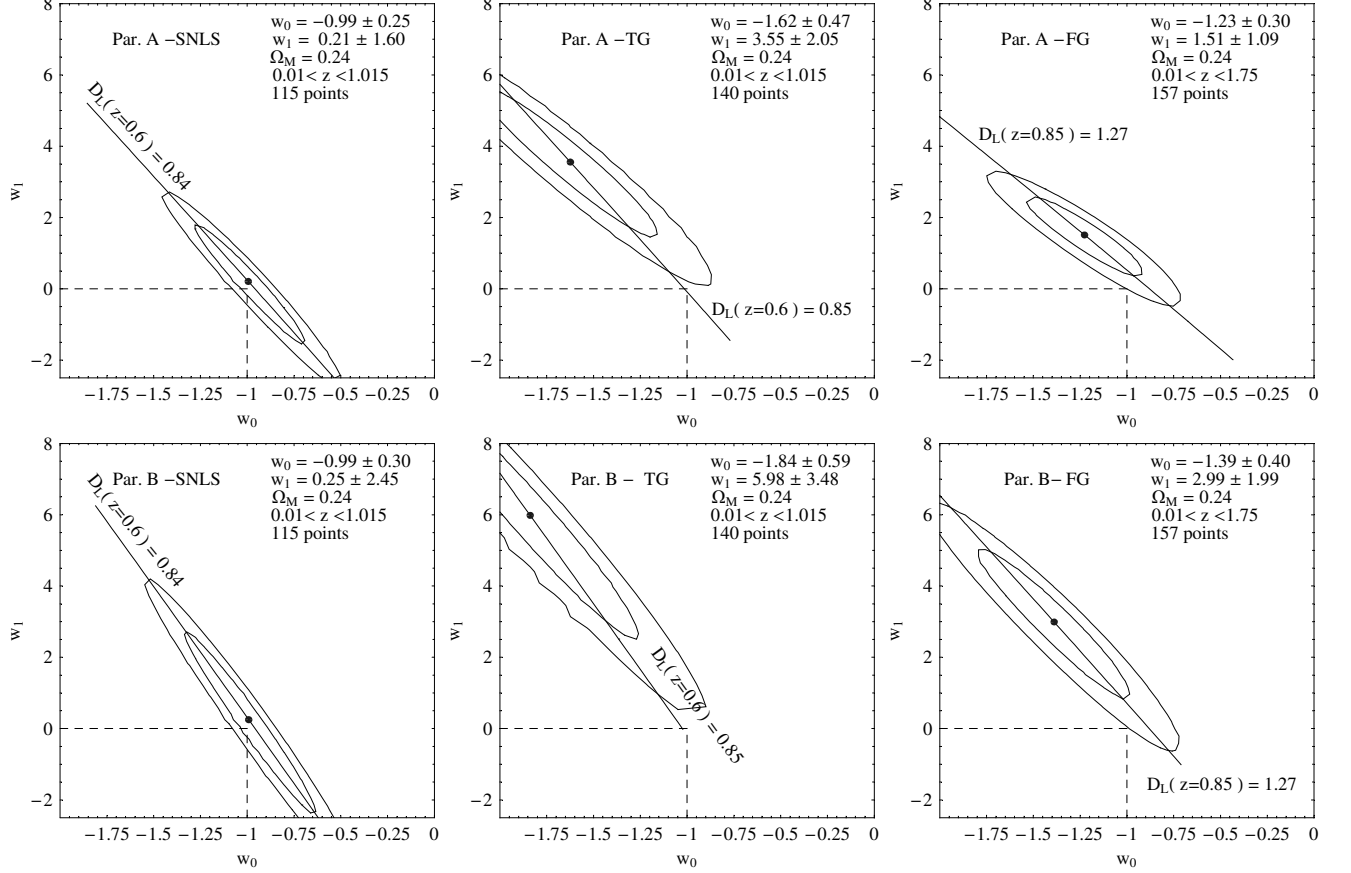


FIG. 2: The 68% and 95% χ^2 confidence contours of parametrizations A and B assuming a flat prior using the datasets SNLS, TG and FG. A prior of $\Omega_{0m} = 0.24$ has been used. The dashed lines intersect at the parameter values of flat LCDM. Notice that for the SNLS, flat LCDM almost coincides with the best fit for both parametrizations.

we find minimizing $\chi^2(\Omega_{0m})$ of eq (1.10)

$$\Omega_{0m}^{SNLS} = 0.26 \pm 0.04 \quad (2.11)$$

$$\Omega_{0m}^{TG} = 0.30 \pm 0.05 \quad (2.12)$$

$$\Omega_{0m}^{FG} = 0.31 \pm 0.04 \quad (2.13)$$

The values of Ω_{0m}^{SNLS} and Ω_{0m}^{FG} are practically identical with the corresponding in the original Refs [4, 5] where the data were first published.

This, along other similar tests, confirms the validity of our analysis.

Even though the cosmological constant with equation of state parameter $w = -1$ is the simplest form of dark energy consistent with the data, the possibility of evolving dark energy models with non-constant $w(z)$ remains a viable alternative which may even provide better fits to the data than LCDM. To address this issue we considered the three parametrizations (A, B, C) of eqs (2.3)-(2.8)

and assuming flatness we constrained their parameters using the three datasets.

Parametrizations A and B reduce to $w(z) = w_0$ in the special case when w does not evolve with time ($w_1 = 0$).

With this prior we construct Table I showing the best fit w_0 value and 1σ errors for each dataset and $\Omega_{0m} = 0.24 - 0.3$. Clearly all datasets are consistent with each other ruling out models with $w > 1/3$ at more than a 10σ confidence level.

Extending the analysis to the full parameter space we construct χ^2 confidence contours in Figs. 2 and 3 assuming a flat prior.

In order to investigate the dependence of our results on the prior of Ω_{0m} we do not marginalize over it. Instead we present the $w_0 - w_1$ confidence contours of parametrizations A and B for the priors $\Omega_{0m} = 0.24$ (Fig. 2) and $\Omega_{0m} = 0.3$ (Fig. 3). The point corresponding to LCDM is also shown in these figures. For parametrization C we have not presented the confidence contours because $H(z)$ becomes complex for regions of parameter space overlap-

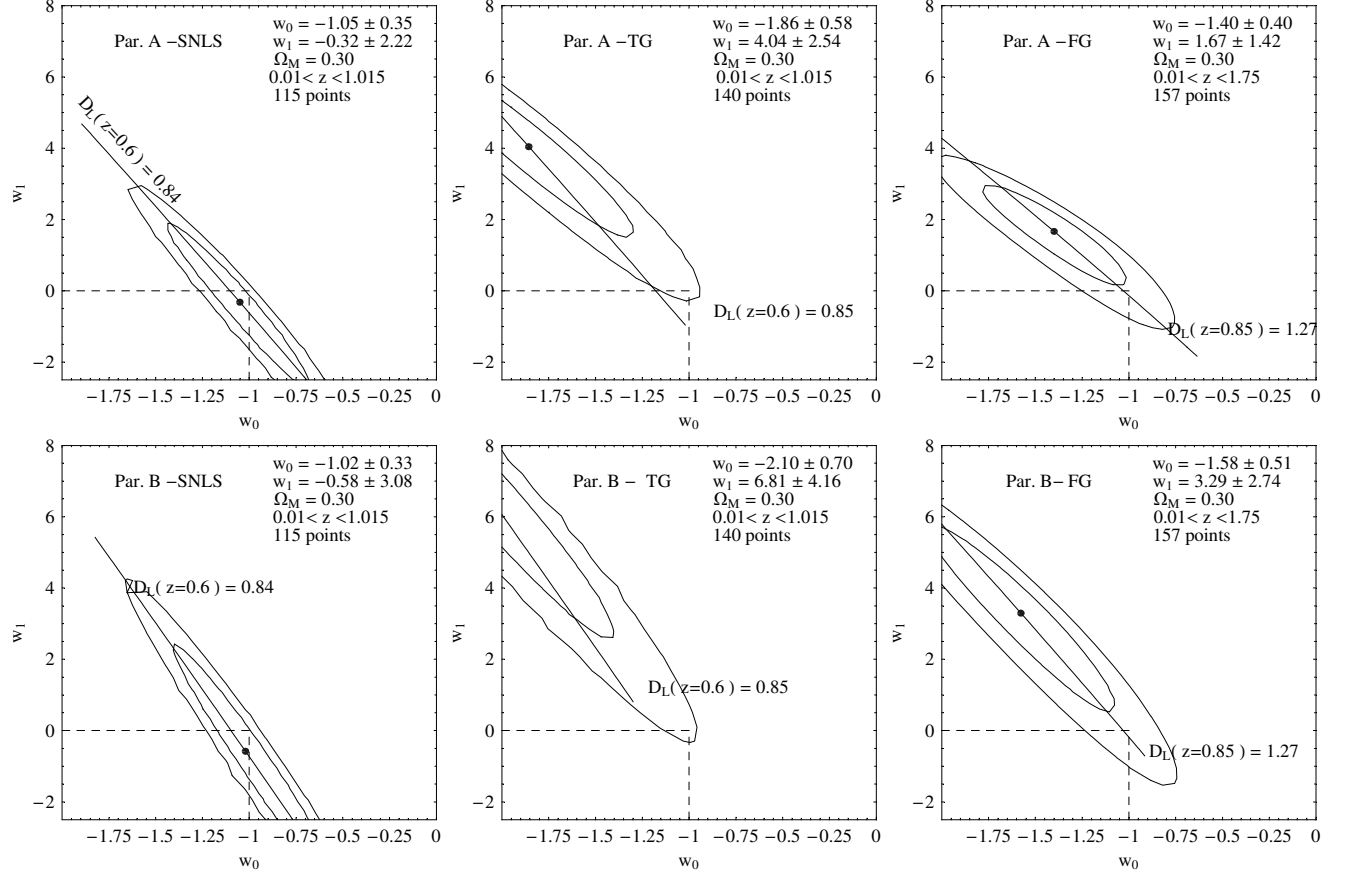


FIG. 3: Same as Fig. 2 but with a prior $\Omega_{0m} = 0.3$.

ing with the 95% confidence contours.

The following comments can be made regarding Figs. 2 and 3.

- The minimal LCDM model ($w_0 = -1$, $w_1 = 0$) appears to be close to the 95% confidence contour in the analyses based on the TG and FG datasets. For the analysis based on the SNLS however, the flat LCDM model is well within the 68% contour and in fact for $\Omega_{0m} = 0.24$ it is almost identical

with the best fit parametrization in both the A and B parametrization cases! Thus LCDM appears to have significantly gained in likelihood compared to dynamical dark energy models in the context of the new SNLS dataset.

TABLE I: The best fit w_0 parameter values for each dataset assuming priors of flatness and $w_1 = 0$.

Matter Density Ω_{0m}	SNLS	TG	FG
0.24	$w_0 = -0.95 \pm 0.09$	$w_0 = -0.89 \pm 0.10$	$w_0 = -0.86 \pm 0.09$
0.30	$w_0 = -1.11 \pm 0.11$	$w_0 = -1.04 \pm 0.12$	$w_0 = -1.02 \pm 0.11$

- The best fit $w(z)$ parametrizations in the context of the FG and the TG datasets, not only are far from the LCDM point ($w_0 = -1$, $w_1 = 0$) (see Figs. 2 and 3) but they also clearly cross the PDL line. This is demonstrated in Fig. 4 where the best fit $w(z)$ are plotted for each dataset and each parametrization with a prior of $\Omega_{0m} = 0.24$.

This crossing of the PDL is not realized for the best fit A, B and C parametrizations in the context of the SNLS dataset. Several authors[16, 18, 22] have been recently motivated by the high likelihood of the PDL crossing indicated by the Gold datasets[23, 24] to explore theoretical models that predict such crossing. It has been shown that this task is not trivial and can not be achieved by a single minimally coupled field[12].

Here we show however that such PDL crossing is not favored by the new SNLS dataset and therefore the motivation for the above papers is weakened. Indeed, phantom[14] dynamical dark energy models with $w_0 < -1$ are not favored by the SNLS dataset in contrast with the Gold dataset that favored such models (see Figs 2 and 3 and Ref. [24, 25]).

- Even though the best fit parameter values are relatively insensitive to the value of Ω_{0m} in the range $0.2 < \Omega_{0m} < 0.3$ the errors are more sensitive increasing with Ω_{0m} . Our results for the best fit parameters of the parametrizations A, B and C are shown in the legends of Figs 2 and 3. For both Ω_{0m} priors the errors of w_1 are much larger compared to those of w_0 . As discussed above, this is a generic feature of the parametrization used and is not related to the particular datasets.

III. DISCUSSION-CONCLUSION

We have performed a comparative analysis of the three most recent and reliable SNIa datasets available in the literature: the Full Gold (FG) dataset (157 data points $0 < z < 1.7$), the Truncated Gold (TG) dataset (140 data points $0 < z < 1$) and the most recent SNLS dataset (115 data points $0 < z < 1$). Our analysis is an extension of our earlier analyses which had focused [25] on the FG and earlier [11] datasets. We have used representative dark energy parametrizations to examine the consistency among the three datasets in constraining the corresponding parameter values. We have found that even though the constraints obtained using the three datasets are consistent with each other at the 95% confidence level, the latest (SNLS) dataset shows distinct trends which are not shared by the other (earlier) datasets. The most characteristic of these trends are the following:

- The best fit dynamical $w(z)$ obtained from the SNLS dataset does not cross the PDL $w = -1$ and remains close to the $w = -1$ line for the whole

redshift range $0 < z < 1$. The LCDM parameters ($w_0 = -1$, $w_1 = 0$) almost coincide with the best fit parameters of the dynamical $w(z)$ parametrizations. Thus, the data do not seem to require and utilize the additional dynamical parameters offered to them. This is an interesting new feature of the data which favors the minimal LCDM model. In contrast, the best fit dynamical $w(z)$ obtained from the Gold datasets (FG and TG) clearly crosses the PDL and departs significantly from the PDL $w = -1$ line (see Fig. 4). According to these datasets the minimal LCDM is consistent but is not favored. It is about 2σ away from the best fit $w(z)$ which crosses the PDL.

- The best fit ($\Omega_{0m}, \Omega_\Lambda$) parameters in a LCDM parametrization without a flat prior show interesting differences between the Gold and the SNLS datasets. In particular, the SNLS favors a flat universe much more than the Gold datasets. However, all three datasets remain consistent with flat LCDM at the 95% confidence level while SCDM is excluded by all datasets at more than 10σ .

The above mild trend differences between the Gold and the SNLS datasets can be summarized by stating that the SNLS hints towards the minimal flat LCDM concordance model more than the Gold datasets. It is an exciting prospect to see whether this trend will continue and get verified by upcoming future SNIa observations.

IV. APPENDIX

Here we give some details of our analysis for both the Gold and the Legacy datasets. The full numerical analysis was performed using Mathematica and it is available at <http://leandros.physics.uoi.gr/snls.htm>

We first describe the method used for the Gold dataset analysis. From eqs. (1.10), (1.11) and (1.12) we find

$$\chi^2(a_1, \dots, a_n) = \sum_{i=1}^N \frac{(\mu_{obs\ i} - 5 \log_{10} D_L(z_i; a_1, \dots, a_n) - \mu_0)^2}{\sigma_i^2} \quad (4.1)$$

where

$$\sigma_i^2 = \sigma_{\mu\ i}^2 + \sigma_{int}^2 + \sigma_v^2 \quad (4.2)$$

is the total error published for the Gold dataset.

The parameter μ_0 is a nuisance parameter but it is independent of the data points and the dataset. This expected independence can be used as consistency test of the data [21]. The minimization with respect to μ_0 can be made trivially by expanding the χ^2 of equation (1.10) with respect to μ_0 as

$$\chi^2(a_1, \dots, a_n) = A - 2\mu_0 B + \mu_0^2 C \quad (4.3)$$

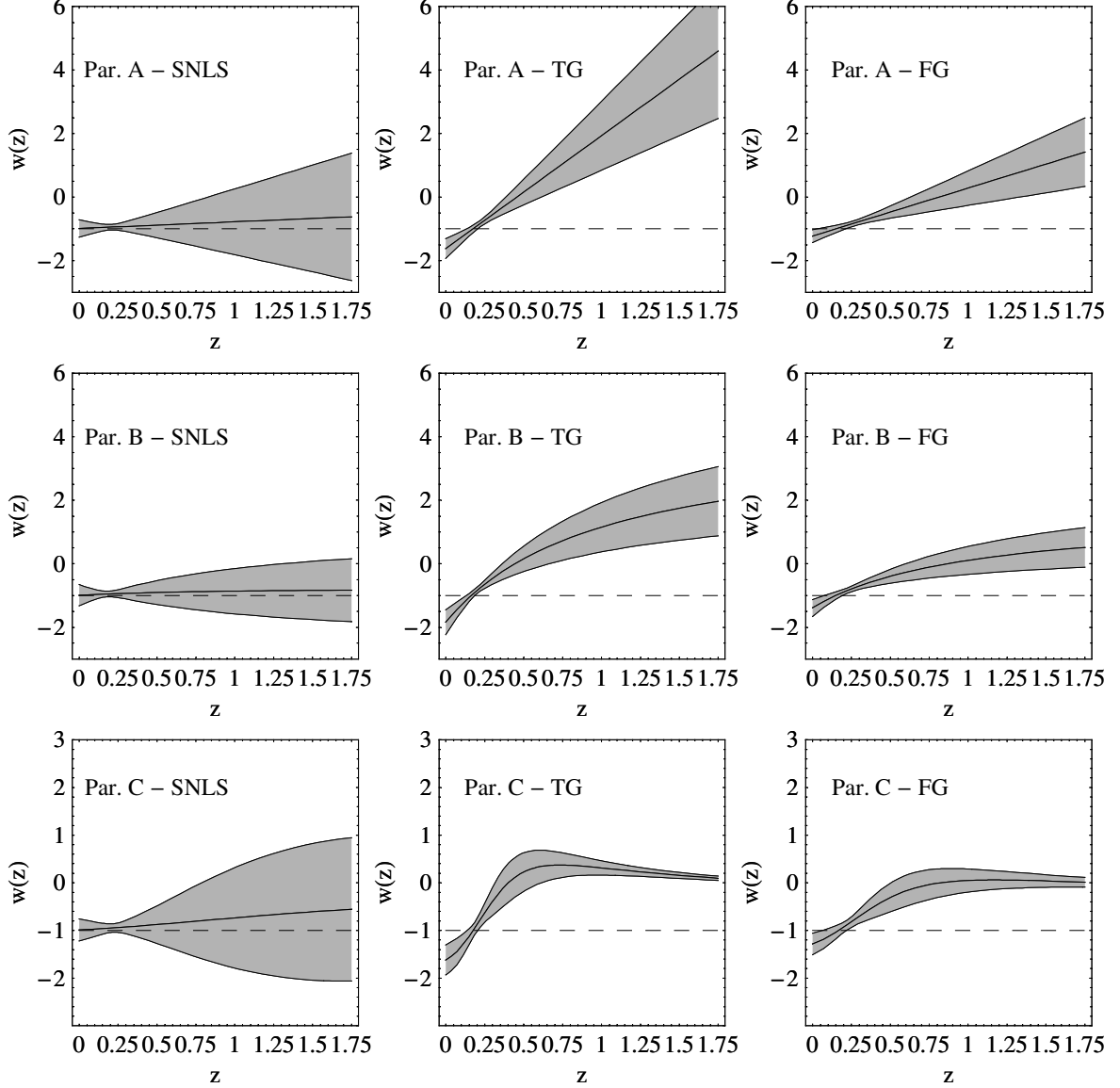


FIG. 4: The best fit $w(z)$ are plotted for each dataset (SNLS, TG and FG) and each parametrization (A, B and C) with a prior of $\Omega_{0m} = 0.24$. The thick solid line represents the best-fit and the light grey contour represents the 1σ confidence level around the best-fit. The dashed horizontal line represents LCDM. Notice that PDL crossing at best fit occurs only for the TG and the FG (Gold) datasets while the best fits of the SNLS dataset almost coincide with LCDM.

where

$$\begin{aligned}
 A(a_1, \dots, a_n) &= \sum_{i=1}^N \frac{(m_{obs}(z_i) - m_{th}(z_i; \mu_0 = 0, a_1, \dots, a_n))^2}{\sigma_{m_{obs}}^2(z_i)} \\
 B(a_1, \dots, a_n) &= \sum_{i=1}^N \frac{(m_{obs}(z_i) - m_{th}(z_i; \mu_0 = 0, a_1, \dots, a_n))}{\sigma_{m_{obs}}^2(z_i)} \\
 C &= \sum_{i=1}^N \frac{1}{\sigma_{m_{obs}}^2(z_i)}
 \end{aligned} \tag{4.4}$$

Equation (4.3) has a minimum for $\mu_0 = B/C$ at

$$\tilde{\chi}^2(a_1, \dots, a_n) = A(a_1, \dots, a_n) - \frac{B(a_1, \dots, a_n)^2}{C} \tag{4.5}$$

Thus instead of minimizing $\chi^2(\mu_0, a_1, \dots, a_n)$ we can minimize $\tilde{\chi}^2(a_1, \dots, a_n)$ which is independent of μ_0 . Obviously $\chi_{min}^2 = \tilde{\chi}_{min}^2$ and this is the approach used. Alternatively we could have performed a uniform marginalization

over the nuisance parameter μ_0 thus obtaining [11, 13, 26]

$$\tilde{\chi}^2(a_1, \dots, a_n) = A(a_1, \dots, a_n) - \frac{B(a_1, \dots, a_n)^2}{C} + \ln(C/2\pi) \quad (4.6)$$

to be minimized with respect to a_1, \dots, a_n . In our Gold dataset analysis we consider the $\tilde{\chi}^2(a_1, \dots, a_n)$ of equation (4.5) which is already minimized with respect to μ_0 . If we marginalized over all values of H_0 , as in Ref. [4], that would just add a constant (see eq.(4.6)) and would not change the results. The minimization of (4.1) was made using the FindMinimum command of Mathematica.

Our analysis of the SNLS dataset proceeded in a somewhat different manner following Ref. [5]. Using equation (1.9) in (1.10) we constructed χ^2 as

$$\chi^2(\alpha, \beta, M + \mu_0, a_1, \dots, a_n) = \sum_{i=1}^N \frac{(\mu_{obs\ i} - 5 \log_{10} D_L(z_i; a_1, \dots, a_n) - \mu_0)^2}{\sigma_{\mu\ i}^2 + \sigma_{int}^2 + \sigma_{v\ i}^2} \quad (4.7)$$

For the distance modulus error we have

$$\sigma_{\mu\ i}^2 = \sigma_{m\ i}^2 + \alpha^2 \sigma_{s\ i}^2 + \beta^2 \sigma_{c\ i}^2 \quad (4.8)$$

Each one of the $\sigma_{m\ i}$, $\sigma_{s\ i}$ and $\sigma_{c\ i}$ has been published in Ref. [5]. The velocity dispersion error σ_v^2 assuming a peculiar velocity dispersion of 300 km/sec may be written as

$$\sigma_{v\ i}^2 = \frac{5 \cdot 10^{-3}}{\ln(10)} \left(\frac{1}{1 + z_i} + \frac{1}{H(z_i) \int_0^{z_i} \frac{dz}{H(z)}} \right)^2 \quad (4.9)$$

The intrinsic dispersion error σ_{int}^2 is initially set to a

value $\sigma_{int} = 0.15$ and then updated with the following three step procedure [5]:

1. Fix the values of α and β in $\sigma_{\mu\ i}^2$ and minimize the χ^2 of eq. (4.8) with $\sigma_{int} = 0.15$. If this fixing is not made, a bias is introduced towards increasing errors during minimization.
2. Change the value of σ_{int} to obtain $\chi^2 = 1$.
3. Use the new value of σ_{int} and minimize again keeping the values of α and β in $\sigma_{\mu\ i}^2$ fixed.

This procedure, with no marginalization over $M + \mu_0$, α , β as described in page 10 of Ref. [5], leads to the best fit values of $M + \mu_0$, α , β , a_1, \dots, a_n .

The errors are evaluated using the covariance matrix of the fitted parameters [27] and the errors on the equation of state $w(z; p_i)$ are given by

$$\sigma_w^2 = \sum_{i=1}^n \left(\frac{\partial w}{\partial p_i} \right) C_{ii} + 2 \sum_{i=1}^n \sum_{j=i+1}^n \left(\frac{\partial w}{\partial p_i} \right) \left(\frac{\partial w}{\partial p_j} \right) C_{ij} \quad (4.10)$$

where p_i are the cosmological parameters and C_{ij} the covariance matrix [28].

Acknowledgements

This work was supported by the program PYTHAGORAS-1 of the Operational Program for Education and Initial Vocational Training of the Hellenic Ministry of Education under the Community Support Framework and the European Social Fund. SN acknowledges support from the Greek State Scholarships Foundation.

-
- [1] D. N. Spergel *et al.* [WMAP Collaboration], *Astrophys. J. Suppl.* **148**, 175 (2003).
 - [2] M. Tegmark *et al.* [SDSS Collaboration], *Phys. Rev. D* **69**, 103501 (2004).
 - [3] Riess A *et al.*, *Astron. J.* **116** 1009 (1998); Perlmutter S *et al.*, *Astroph. J.* **517** 565 (1999); S. Perlmutter *et al.*, *Nature (London)* **391**, 51(1998); Tonry, J L *et al.*, 2003 *Astroph. J.* **594** 1; Barris, B *et al.*, 2004 *Astroph. J.* **602** 571; Knop R *et al.*, 2003 *Astroph. J.* **598** 102;
 - [4] A. G. Riess *et al.* [Supernova Search Team Collaboration], *Astrophys. J.* **607**, 665 (2004).
 - [5] P. Astier *et al.*, arXiv:astro-ph/0510447.
 - [6] V. Sahni, arXiv:astro-ph/0403324; D. Huterer and M. S. Turner, *Phys. Rev. D* **64**, 123527 (2001) [arXiv:astro-ph/0012510];
 - [7] V. Sahni and A. A. Starobinsky, *Int. J. Mod. Phys. D* **9**, 373 (2000) [arXiv:astro-ph/9904398]; S. M. Carroll, *Living Rev. Rel.* **4**, 1 (2001) [arXiv:astro-ph/0004075]; P. J. E. Peebles and B. Ratra, *Rev. Mod. Phys.* **75**, 559 (2003) [arXiv:astro-ph/0207347]; T. Padmanabhan, *Phys. Rept.* **380**, 235 (2003) [arXiv:hep-th/0212290].
 - [8] B. Ratra and P.J.E. Peebles, *Phys. Rev. D* **37**, 3406 (1988); *Rev. Mod. Phys.* **75**, 559 (2003) [arXiv:astro-ph/0207347]; C. Wetterich, *Nucl. Phys. B* **302**, 668(1988); P.G.Ferreira and M. Joyce, *Phys. Rev. D* **58**, 023503(1998).
 - [9] B. Boisseau, G. Esposito-Farese, D. Polarski and A. A. Starobinsky, *Phys. Rev. Lett.* **85**, 2236 (2000) [arXiv:gr-qc/0001066]; F. Perrotta, C. Baccigalupi and S. Matarrese, *Phys. Rev. D* **61**, 023507 (2000) [arXiv:astro-ph/9906066]; N. Bartolo and M. Pietroni, *Phys. Rev. D* **61**, 023518 (2000) [arXiv:hep-ph/9908521]; L. Perivolaropoulos, arXiv:astro-ph/0504582, *JCAP* **10**, 001 (2005); L. Perivolaropoulos, *Phys. Rev. D* **67**, 123516 (2003) [arXiv:hep-ph/0301237]; D.F.Torres, *Phys. Rev. D* **66**, 043522(2002); L. Perivolaropoulos and C. Sourdis, *Phys. Rev. D* **66**, 084018 (2002) [arXiv:hep-ph/0204155].
 - [10] D. Huterer and M. S. Turner, *Phys. Rev. D* **64**, 123527 (2001) [arXiv:astro-ph/0012510].
 - [11] S. Nesseris and L. Perivolaropoulos, *Phys. Rev. D* **70**, 043531 (2004) [arXiv:astro-ph/0401556].
 - [12] A. Vikman, *Phys. Rev. D* **71**, 023515 (2005) [arXiv:astro-ph/0407107].

- [13] L. Perivolaropoulos, Phys. Rev. D **71**, 063503 (2005) [arXiv:astro-ph/0412308].
- [14] R. R. Caldwell, Phys. Lett. B **545**, 23 (2002) [arXiv:astro-ph/9908168]; P. Singh, M. Sami and N. Dadhich, Phys. Rev. D **68**, 023522 (2003) [arXiv:hep-th/0305110]; V. B. Johri, Phys. Rev. D **70**, 041303 (2004) [arXiv:astro-ph/0311293]; B. McInnes, astro-ph/0210321.
- [15] C. Armendariz-Picon, V. Mukhanov and P. J. Steinhardt, Phys. Rev. D **63**, 103510 (2001) [arXiv:astro-ph/0006373]; R. J. Scherrer, Phys. Rev. Lett. **93**, 011301 (2004) [arXiv:astro-ph/0402316].
- [16] L. Perivolaropoulos, JCAP **10**, 001 (2005), arXiv:astro-ph/0504582.
- [17] S. Tsujikawa, arXiv:astro-ph/0508542.
- [18] X. F. Zhang, H. Li, Y. S. Piao and X. M. Zhang, arXiv:astro-ph/0501652; M. Z. Li, B. Feng and X. M. Zhang, arXiv:hep-ph/0503268; G. B. Zhao, J. Q. Xia, M. Li, B. Feng and X. Zhang, arXiv:astro-ph/0507482; B. Feng, X. L. Wang and X. M. Zhang, Phys. Lett. B **607**, 35 (2005) [arXiv:astro-ph/0404224].
- [19] A. Anisimov, E. Babichev and A. Vikman, JCAP **0506**, 006 (2005) [arXiv:astro-ph/0504560];
- [20] D. Huterer and A. Cooray, Phys. Rev. D **71**, 023506 (2005) [arXiv:astro-ph/0404062].
- [21] T. R. Choudhury and T. Padmanabhan, Astron. Astrophys. **429**, 807 (2005) [arXiv:astro-ph/0311622].
- [22] W. Hu, Phys. Rev. D **71**, 047301 (2005) [arXiv:astro-ph/0410680].
- [23] U. Alam, V. Sahni and A. A. Starobinsky, JCAP **0406**, 008 (2004) [arXiv:astro-ph/0403687].
- [24] U. Alam, V. Sahni, T. D. Saini and A. A. Starobinsky, Mon. Not. Roy. Astron. Soc. **354**, 275 (2004) [arXiv:astro-ph/0311364]; Y. Wang and P. Mukherjee, Astrophys. J. **606**, 654 (2004) [arXiv:astro-ph/0312192];
- [25] R. Lazkoz, S. Nesseris and L. Perivolaropoulos, arXiv:astro-ph/0503230.
- [26] E. Di Pietro and J. F. Claeskens, Mon. Not. Roy. Astron. Soc. **341**, 1299 (2003) [arXiv:astro-ph/0207332].
- [27] W. H. Press *et. al.*, 'Numerical Recipes', Cambridge University Press (1994).
- [28] U. Alam, V. Sahni, T. D. Saini and A. A. Starobinsky, arXiv:astro-ph/0406672.